Journal of Applied Analysis and Computation
Volume 13, Number 3, June 2023, 1304–1320
Website:http://www.jaac-online.com
DOI:10.11948/20220123

PARAMETER INDEPENDENT SCHEME FOR SINGULARLY PERTURBED PROBLEMS INCLUDING A BOUNDARY TURNING POINT OF MULTIPLICITY ≥ 1

Parvin Kumari[1,†], Devendra Kumar[2], Higinio Ramos[3,4]

Abstract A numerical scheme is developed for parabolic singularly perturbed boundary value problems, including multiple boundary turning points at the left endpoint of the spatial direction. The highest order derivative of these problems is multiplied by a small parameter $\varepsilon\,(0 < \varepsilon \ll 1)$, and when it is close to zero, the solution exhibits a parabolic type boundary layer near the left lateral surface of the domain of consideration. Thus, large oscillations appear when classical/standard numerical methods are used to solve the problem, and one cannot achieve the expected accuracy. Thus, the Crank-Nicolson scheme on a uniform mesh in the temporal direction and an upwind scheme on a Shishkin-type mesh in the spatial direction is constructed. The theoretical analysis shows that the method converges irrespective of the size of ε with accuracy $\mathcal{O}((\Delta t)^2 + N^{-1}\ln N)$. Three test examples are presented to verify that the computational results agree with the theoretical ones.

Keywords Singularly perturbed parabolic problems, Shishkin-type mesh, multiple boundary turning points, parameter-uniform convergence.

MSC(2010) 65L10, 65L12, 65L20, 65L70.

1. Introduction

Let $\Omega = (0,1)$, $\Lambda = (0,T]$, $\mathcal{D} = \Omega \times \Lambda$, with boundary $\Gamma = \Gamma_l \cup \Gamma_b \cup \Gamma_r$, where $\Gamma_l = \{(0,t)\,|\,0 \leq t \leq T\}$, $\Gamma_b = \{(x,0)\,|\,0 \leq x \leq 1\}$ and $\Gamma_r = \{(1,t)\,|\,0 \leq t \leq T\}$ are the left, bottom and the right boundaries of $\mathcal{D}$. In this paper, we consider the following problem

$$L\psi(x,t) \equiv -\psi_t + \varepsilon\psi_{xx} + a(x,t)\psi_x - b(x,t)\psi = f(x,t), \quad (x,t) \in \mathcal{D}, \tag{1.1a}$$

$$\psi(x,0) = \psi_b(x), \quad x \in \overline{\Omega}, \tag{1.1b}$$

$$\psi(0,t) = \psi_l(t), \quad t \in \overline{\Lambda}, \tag{1.1c}$$

†The corresponding author.
Email: parvinbedwal@gmail.com(P. Kumari),
[1]Department of Mathematics, School of Basic Sciences Central University of Haryana, Mahendergarh-123029, India
[2]Department of Mathematics, Birla Institute of Technology and Science, Pilani, Rajasthan-333031, India
[3]Scientific Computing Group, Universidad de Salamanca, Plaza de la Merced, 37008 Salamanca, Spain
[4]Escuela Politécnica Superior de Zamora, Campus Viriato, 49029 Zamora, Spain

$$\psi(1,t) = \psi_r(t), \quad t \in \overline{\Lambda}, \tag{1.1d}$$

where $0 < \varepsilon \ll 1$ is a diffusion parameter. The following assumptions are made, which ensure that the problem (1.1) has a unique solution.

- The functions $a(x,t),\ b(x,t),\ f(x,t)$ in $\overline{\mathcal{D}}$ and $\psi_l(t),\ \psi_r(t),\ \psi_b(x)$ are smooth enough and bounded.
- $a(x,t) = a^*(x,t)x^p,\ p \geq 1$ where $a^*(x,t)$ is smooth and satisfies $a^*(x,t) \geq \alpha > 0,\ (x,t) \in \overline{\mathcal{D}}$.
- $b(x,t) \geq \beta > 0,\ (x,t) \in \overline{\mathcal{D}}$.
- The corresponding compatibility conditions at the corners are satisfied.

These problems arise for instance, in transport phenomena [17], laminar flow [16], heat flow [5], etc. For the applications of problems with multiple boundary turning points ($p > 1$), the readers are referred to [16]. The layer behavior of the singularly perturbed boundary value problems (SPBVPs) is characterized differently according to the sign of $a(x,t)$. If $a(x,t)$ is positive throughout $\overline{\mathcal{D}}$, a regular/exponential boundary layer appears near the left lateral surface of the domain. Moreover, if $a(x,t)$ is negative throughout $\overline{\mathcal{D}}$, a regular/exponential boundary layer appears near the right lateral surface of the domain. On the other hand, for $a(x,t)$ identically zero in $\overline{\mathcal{D}}$, there are parabolic boundary layers at both ends. Although, in our problem, the form of $a(x,t)$ is different from the above cases, a parabolic boundary layer appears in the solution near the left lateral surface Γ_l. The boundary layer behavior of the SPBVPs leads to the failure of the classical/standard numerical methods unless an unacceptably large number of mesh points is used, which is very costly. In this case, it is convenient to have a convergent method irrespective of the size of ε in some discrete norm. For detailed discussions on the parameter-uniform numerical methods, the readers are referred to Farrell *et al.* [3], Miller *et al.* [12], and Roos *et al.* [14] (and the references therein).

The numerical study of the single boundary turning point problems for ordinary differential equations has been considered by many researchers [9–11, 14, 18–20]. Liseikin [11] constructed a first-order parameter-uniform scheme in the discrete maximum norm on a uniform mesh by using some transformation. Vulanović [18] used a Bakhvalov-type mesh to find the solution of mildly non-linear SPBVPs with a turning point, showing the parameter-uniform convergence in a discrete ℓ_1-norm. Later, Vulanović and Lin [19] extended the result of [18] for the singularly perturbed quasi-linear BVP with the attractive turning point. To solve SPBVPs with multiple boundary turning points, Vulanović and Farrell [20] constructed an exponentially fitted scheme. They suggested using a modified scheme on a special discretization mesh to improve the order of convergence from first-order to second-order. Linß and Vulanović [9] constructed upwind schemes in the discrete ℓ_1-norm for the semi-linear convection-diffusion problem with the attractive boundary turning point. There are only a few articles on the numerical solution to the problem (1.1). For instance, based on the finite differences and using the classical grid approximations [15], Shishkin [17] constructed parameter-uniform convergent schemes for the solution of (1.1). In [2], to solve a time-dependent convection-diffusion SPBVPs for PDEs with a boundary turning point, Dunne *et al.* developed a parameter-uniform first-order upwind finite difference scheme on a fitted mesh. To obtain a parameter-uniform convergence for the solution of (1.1), Gupta and Kadalbajoo [4] used B-splines on a Shishkin mesh.

The summary of the paper is as follows. Some *a priori* estimates are established in Section 2. In particular, some bounds on the derivatives of the solution and the minimum principle are established. Furthermore, sharper bounds are given on the smooth and singular components and their derivatives. The temporal semi-discretization and the local and global error estimates in the temporal direction are presented in Section 3. The discretization of the system of ODEs obtained in the temporal semi-discretization by using a finite difference scheme on a Shishkin-type mesh is also constructed in this section. The main result of the convergence is proved in Section 4, followed by some numerical experiments and discussions in Section 5. Finally, some concluding remarks and future scope are included in Section 6.

2. Continuous Problem

In this section, we establish some *a priori* results like minimum principle, stability estimate, and some bound estimates of the derivatives. Throughout the paper, the norm will be taken as the maximum norm, and C will denote a generic constant independent of the perturbation parameter and the grid points. The following minimum principle is straightforward and can be proved by following the approach given in [7].

Lemma 2.1. *Let $\Phi \in C^{2,1}(\overline{\mathcal{D}})$ be non-negative on Γ and $L\Phi$ non-positive in the interior of $\mathcal{D}$. Then, Φ is non-negative throughout $\overline{\mathcal{D}}$.*

The following stability lemma establishes an ε-uniform bound on the solution $\psi(x,t)$ of (1.1).

Lemma 2.2. *The solution $\psi(x,t)$ of (1.1) satisfies*

$$\|\psi\|_{\overline{\mathcal{D}}} \leq \|\psi\|_{\Gamma} + \frac{\|f\|_{\overline{\mathcal{D}}}}{\beta}.$$

Proof. Consider the functions $\Pi^{\pm}(x,t) = \|\psi\|_{\Gamma} + \frac{\|f\|_{\overline{\mathcal{D}}}}{\beta} \pm \psi(x,t)$. We have

$$\Pi^{\pm}(0,t) = \|\psi\|_{\Gamma} + \frac{\|f\|_{\overline{\mathcal{D}}}}{\beta} \pm \psi(0,t) \geq \|\psi\|_{\Gamma} \pm \psi(0,t) \geq 0,$$

$$\Pi^{\pm}(1,t) = \|\psi\|_{\Gamma} + \frac{\|f\|_{\overline{\mathcal{D}}}}{\beta} \pm \psi(1,t) \geq \|\psi\|_{\Gamma} \pm \psi(1,t) \geq 0,$$

$$\Pi^{\pm}(x,0) = \|\psi\|_{\Gamma} + \frac{\|f\|_{\overline{\mathcal{D}}}}{\beta} \pm \psi(x,0) \geq \|\psi\|_{\Gamma} \pm \psi(x,0) \geq 0.$$

Also, at all interior points (x,t) of $\mathcal{D}$ it is

$$\begin{aligned} L\Pi^{\pm}(x,t) &= -b(x,t)\left[\|\psi\|_{\Gamma} + \frac{\|f\|_{\overline{\mathcal{D}}}}{\beta}\right] \pm L\psi(x,t) \\ &\leq -\beta\|\psi\|_{\Gamma} - \|f\|_{\overline{\mathcal{D}}} \pm f(x,t) \\ &\leq -\|f\|_{\overline{\mathcal{D}}} \pm f(x,t) \\ &\leq 0. \end{aligned}$$

The proof is completed using the minimum principle in Lemma 2.1. □

The following theorem can be proved by using the arguments by Kellog and Tsan in [6].

Theorem 2.1. *The mixed derivatives of the solution $\psi(x,t)$ of (1.1) satisfy the following bounds*

$$\left\| \frac{\partial^{i+j}\psi}{\partial x^i \partial t^j} \right\|_{\overline{\mathcal{D}}} \leq C\left(1+\varepsilon^{-i/2}e^{-x\sqrt{\beta/\varepsilon}}\right), \quad 0 \leq i+3j \leq 4.$$

3. Description of the Numerical Scheme

To discretize the problem in the temporal direction, we divide the interval $[0,T]$ into M subintervals, each of width $\Delta t = T/M$. Thus, the mesh in the temporal direction is

$$\Lambda^M = \{t_j = j\Delta t : \ j = 0,1,\ldots,M\}.$$

Then, on $\Omega \times \Lambda^M$ problem (1.1) is discretized as follows:

$$\begin{aligned}
&-D_t^- u^{j+1}(x)+\varepsilon(u_{xx})^{j+1/2}+a^{j+1/2}(x)(u_x)^{j+1/2}-b^{j+1/2}(x)u^{j+1/2}(x)=f^{j+1/2}(x),\\
&x \in \Omega,\ 0 \leq j \leq M-1,\\
&u^{j+1}(0)=\psi_l(t_{j+1}),\ u^{j+1}(1)=\psi_r(t_{j+1}), \quad 0 \leq j \leq M-1,\\
&u^0(x)=\psi_b(x), \quad x \in \Omega,
\end{aligned}$$

where $u^{j+1}(x)$ is the approximation of $\psi(x,t_{j+1})$, $D_t^- z^j(x)=\frac{z^j(x)-z^{j-1}(x)}{\Delta t}$, $z^{j+1/2}(x)=\frac{z^{j+1}(x)+z^j(x)}{2}$, and $f^{j+1/2}(x)=\frac{f^{j+1}(x)+f^j(x)}{2}$. The discretized problem can be rewritten as

$$\begin{cases}
\hat{L}u^{j+1}(x)=g(x,t_{j+1}), & x \in \Omega,\ 0 \leq j \leq M-1,\\
u^{j+1}(0)=\psi_l(t_{j+1}),\ u^{j+1}(1)=\psi_r(t_{j+1}), & 0 \leq j \leq M-1,\\
u^0(x)=\psi_b(x), \quad x \in \Omega,
\end{cases} \tag{3.1}$$

where

$$\begin{aligned}
&\hat{L} \equiv \frac{\varepsilon}{2}\frac{d^2}{dx^2}+\frac{a^{j+1/2}(x)}{2}\frac{d}{dx}-\frac{c^{j+1/2}(x)}{2}I,\\
&g(x,t_{j+1})=f^{j+1/2}(x)-\frac{\varepsilon}{2}(u_{xx})^j(x)-\frac{a^{j+1/2}(x)}{2}(u_x)^j(x)+\frac{d^{j+1/2}(x)}{2}u^j(x),\\
&d^{j+1/2}(x)=b^{j+1/2}(x)-\frac{2}{\Delta t}, \quad c^{j+1/2}(x)=b^{j+1/2}(x)+\frac{2}{\Delta t}.
\end{aligned}$$

Lemma 3.1. *If $\Phi^{j+1}(0)$ and $\Phi^{j+1}(1)$ are non-negative and $\hat{L}\Phi^{j+1} \leq 0$ on Ω, then $\Phi^{j+1}(x) \geq 0$ on $\overline{\Omega}$.*

Proof. Suppose there exists $s \in \Omega$, such that $\Phi^{j+1}(s) = \min\limits_{x\in\Omega}\Phi^{j+1}(x) < 0$. It follows that $(\Phi^{j+1})'(s)=0$ and $(\Phi^{j+1})''(s) \geq 0$. Then, we have

$$\hat{L}\Phi^{j+1}(s)=\frac{\varepsilon}{2}(\Phi^{j+1})''(s)+\frac{a^{j+1/2}(s)}{2}(\Phi^{j+1})'(s)-\frac{c^{j+1/2}(s)}{2}\Phi^{j+1}(s)>0,$$

since $c^{j+1/2}(s)=b^{j+1/2}(s)+\frac{2}{\Delta t} \geq \beta+\frac{2}{\Delta t}>0$. Thus, the proof is completed by contradiction. □

As a result of Lemma 3.1, the operator $\hat{L}$ has the following stability feature.

Lemma 3.2. *If $\Phi^{j+1}(0)$ and $\Phi^{j+1}(1)$ are non negative, then*

$$|\Phi^{j+1}(x)| \leq \max\{|\Phi^{j+1}(0)|, |\Phi^{j+1}(1)|\} + T \max_{x\in\Omega} \frac{|\hat{L}\Phi^{j+1}(x)|}{\beta}, \ x \in \overline{\Omega}.$$

The local truncation error e_{j+1} of the temporal semi-discretization, defined as $e_{j+1}(x) = \hat{L}\psi(x, t_{j+1}) - g^{j+1}(x)$ satisfies the following estimate

Lemma 3.3. *The local truncation error estimate is given by*

$$\|e_{j+1}\| \leq C(\Delta t)^3, \ j = 0, 1, \ldots, M-1.$$

Proof. Using Taylor's theorem, we have

$$\psi(x, t_{j+1}) = \psi(x, t_{j+1/2}) + \frac{\Delta t}{2}\psi_t(x, t_{j+1/2}) + \frac{(\Delta t)^2}{8}\psi_{tt}(x, t_{j+1/2}) + O((\Delta t)^3),$$
$$\psi(x, t_j) = \psi(x, t_{j+1/2}) - \frac{\Delta t}{2}\psi_t(x, t_{j+1/2}) + \frac{(\Delta t)^2}{8}\psi_{tt}(x, t_{j+1/2}) + O((\Delta t)^3).$$

On subtracting, it gives

$$\begin{aligned}
&\frac{\psi(x, t_{j+1}) - \psi(x, t_j)}{\Delta t} \\
&= \psi_t\left(x, t_{j+\frac{1}{2}}\right) + O((\Delta t)^2) \\
&= \varepsilon\psi_{xx}(x, t_{j+1/2}) + a(x, t_{j+1/2})\psi_x(x, t_{j+1/2}) - b(x, t_{j+1/2})\psi(x, t_{j+1/2}) \\
&\quad - f(x, t_{j+1/2}) + O((\Delta t)^2),
\end{aligned}$$

where $a(x, t_{j+1/2}) = \frac{a(x,t_{j+1})+a(x,t_j)}{2}$, etc. So, we can see that the local error is the solution of

$$\hat{L}e_{j+1} = O((\Delta t)^3),$$
$$e_{j+1}(0) = e_{j+1}(1) = 0.$$

Hence, by using Lemma 3.2, we get the required result. □

Furthermore, the following estimate for the global error $E_j = \psi(x, t_j) - u^j(x)$ of the time semi-discretization can be proved using the local error estimates and an application of Lemma 3.3.

Theorem 3.1. *The global error estimate satisfies*

$$\|E_j\| \leq C(\Delta t)^2, \quad 0 \leq j \leq M.$$

The following estimates on $u^{j+1}(x)$ and its derivatives can be proved by following the technique given in [6].

Theorem 3.2.

$$\left|\frac{d^k u^{j+1}(x)}{dx^k}\right| \leq C(1 + \varepsilon^{-k/2}\exp(-x\sqrt{\beta/\varepsilon})), \quad k = 0, 1, 2, 3.$$

We further decompose the solution $u^{j+1}(x)$ as

$$u^{j+1}(x) = u_r(x, t_{j+1}) + u_s(x, t_{j+1}), \quad x \in \overline{\Omega},$$

where the regular and singular components $u_r(x, t_{j+1})$ and $u_s(x, t_{j+1})$ satisfy the following estimates.

Theorem 3.3.

$$\left|\frac{d^k u_r(x,t_{j+1})}{dx^k}\right| \le C(1+\varepsilon^{(1-k)/2}),\ \ k=0,1,2,$$
$$\left|\frac{d^k u_s(x,t_{j+1})}{dx^k}\right| \le C\varepsilon^{-k/2}\exp(-x\sqrt{\beta/\varepsilon}),\ \ k=0,1,2,3.$$

Proof. The proof can be readily obtained following steps like those given in [13]. □

Now we discretize the problem (3.1) in the spatial direction by using an upwind scheme on a predefined Shishkin mesh. The appearance of the boundary layer suggests us to increase the density of the points in the neighborhood of the layer region. This type of mesh can be constructed by taking $\overline{\Omega} = \Omega_1 \cup \Omega_2$, where $\Omega_1 = [0,\tau],\ \Omega_2 = (\tau,1]$, and the transition parameter τ is given by

$$\tau = \min\{1/2, \tau^*\sqrt{\varepsilon}\,\ln N\}.$$

Here $N \ge 2$ is an even integer and τ^* is a constant that depends on $b(x,t)$ and should be chosen as $\tau^* \ge \frac{1}{\sqrt{\beta}}$. We place $N/2$ points in each of the subintervals $[0,\tau]$ and $(\tau,1]$. Clearly, the mesh $\Omega^N = \{x_i\}_{i=0}^N$ generated in this way is dense in the layer region and is given by

$$x_i = \begin{cases} \frac{2\tau}{N} i, & i = 0,1,\ldots,N/2, \\ \tau + \frac{2(1-\tau)}{N}\left(i - \frac{N}{2}\right), & i = N/2+1,\ldots,N, \end{cases}$$

and the mesh spacing is given by

$$h_i = x_i - x_{i-1} = \begin{cases} \frac{2\tau}{N}, & i = 1,2,\ldots,N/2, \\ \frac{2(1-\tau)}{N}, & i = N/2+1,\ldots,N. \end{cases}$$

Thus $\mathcal{D}^{N,M} = \Omega^N \times \Lambda^M$ is our fully discretized mesh and $\Gamma^{N,M} = \overline{\mathcal{D}}^{N,M} \cap \Gamma$ is the boundary of the mesh. Introducing the operators

$$D_x^- \mu_i^j = \frac{\mu_i^j - \mu_{i-1}^j}{h_i},\ D_x^+ \mu_i^j = \frac{\mu_{i+1}^j - \mu_i^j}{h_{i+1}},\ \delta_x^2 \mu_i^j = \frac{(D_x^+ - D_x^-)\mu_i^j}{\hbar_i},$$

where $\hbar_i = \frac{h_i + h_{i+1}}{2}$, the full discretization of (3.1) on $\mathcal{D}^{N,M}$ is given by

$$\begin{cases} \mathcal{L}^N \widetilde{\psi}(x_i) = \widetilde{g}(x_i), & x_i \in \Omega^N, \\ \widetilde{\psi}(x_0) = \psi_l(t_{j+1}), & \widetilde{\psi}(x_N) = \psi_r(t_{j+1}),\ 0 \le j \le M-1, \end{cases} \tag{3.2}$$

where $\widetilde{\psi}(x_i) \approx u^{j+1}(x_i)$ and

$$\widetilde{g}(x_i) = f^{j+1/2}(x_i) - \frac{\varepsilon}{2}\delta_x^2 u^j(x_i) - \frac{a^{j+1/2}(x_i)}{2} D^- u^j(x_i) + \frac{d^{j+1/2}(x_i)}{2} u^j(x_i).$$

The midpoint upwind operator $\mathcal{L}^N$ is given by

$$\mathcal{L}^N \widetilde{\psi} :\equiv \frac{\varepsilon}{2}\delta_x^2 \widetilde{\psi} + \frac{a^{j+1/2}(x_i)}{2} D^- \widetilde{\psi} - \frac{c^{j+1/2}(x_i)}{2}\widetilde{\psi}.$$

4. Convergence analysis

The main theorem is proved in this section. First, we demonstrate two lemmas that will be used to establish the main result.

Lemma 4.1. *Assume that* $\widetilde{\Phi}(x_0) \geq 0, \widetilde{\Phi}(x_N) \geq 0$ *and* $\mathcal{L}^N\widetilde{\Phi}(x_i) \leq 0$ *for all* $x_i \in \Omega^N$. *Then* $\widetilde{\Phi}(x_i) \geq 0$ *for all* $x_i \in \Omega^N$.

Proof. Suppose $\widetilde{\Phi}(\xi_i) = \min\limits_{x_i\in\Omega^N} \widetilde{\Phi}(x_i) < 0$ for some $\xi_i \in \Omega^N$. Then, we have

$$\begin{aligned}
\mathcal{L}^N\widetilde{\Phi}(\xi_i) &= \frac{\varepsilon}{2}\delta_x^2\widetilde{\Phi}(\xi_i) + \frac{a^{j+1/2}(\xi_{i-\frac{1}{2}})}{2}D^-\widetilde{\Phi}(\xi_i) - \frac{c^{j+1/2}(\xi_{i-\frac{1}{2}})}{2}\widetilde{\Phi}(\xi_i)\\
&= \frac{\varepsilon}{2\hbar_i}\left(\frac{\widetilde{\Phi}(\xi_{i+1}) - \widetilde{\Phi}(\xi_i)}{h_{i+1}} - \frac{\widetilde{\Phi}(\xi_i) - \widetilde{\Phi}(\xi_{i-1})}{h_i}\right)\\
&\quad + \frac{a^{j+1/2}(\xi_{i-\frac{1}{2}})}{2}\left(\frac{\widetilde{\Phi}(\xi_i) - \widetilde{\Phi}(\xi_{i-1})}{h_i}\right) - \frac{c^{j+1/2}(\xi_{i-\frac{1}{2}})}{2}\widetilde{\Phi}(\xi_i)\\
&> 0.
\end{aligned}$$

Hence, the proof is completed by contradiction. □

Lemma 4.2. *Assume that* $\widetilde{\Phi}(x_0) = \widetilde{\Phi}(x_N) = 0$. *Then, for* $\Delta t < 1$

$$|\widetilde{\Phi}(x_i)| \leq \max_{x_i\in\Omega^N} |\mathcal{L}^N\widetilde{\Phi}(x_i)|,\ x_i \in \Omega^N.$$

Proof. For the barrier functions $\Psi^{\pm}(x_i) = \max\limits_{x_i\in\Omega^N} |\mathcal{L}^N\widetilde{\Phi}(x_i)| \pm \widetilde{\Phi}(x_i)$, we have

$$\begin{aligned}
\Psi^{\pm}(x_0) &= \max_{x_i\in\Omega^N} |\mathcal{L}^N\widetilde{\Phi}(x_i)| \pm \widetilde{\Phi}(x_0) = \max_{x_i\in\Omega^N} |\mathcal{L}^N\widetilde{\Phi}(x_i)| \geq 0,\\
\Psi^{\pm}(x_N) &= \max_{x_i\in\Omega^N} |\mathcal{L}^N\widetilde{\Phi}(x_i)| \pm \widetilde{\Phi}(x_N) = \max_{x_i\in\Omega^N} |\mathcal{L}^N\widetilde{\Phi}(x_i)| \geq 0.
\end{aligned}$$

Also,

$$\begin{aligned}
\mathcal{L}^N\Psi^{\pm}(x_i) &= \mathcal{L}^N\left[\max_{x_i\in\Omega^N} |\mathcal{L}^N\widetilde{\Phi}(x_i)| \pm \widetilde{\Phi}(x_i)\right]\\
&= -\frac{c^{j+1/2}(x_{i-1/2})}{2}\max_{x_i\in\Omega^N} |\mathcal{L}^N\widetilde{\Phi}(x_i)| \pm \mathcal{L}^N\widetilde{\Phi}(x_i)\\
&= -\frac{1}{2}\left(b^{j+1/2}(x_{i-1/2}) + \frac{2}{\Delta t}\right)\max_{x_i\in\Omega^N} |\mathcal{L}^N\widetilde{\Phi}(x_i)| \pm \mathcal{L}^N\widetilde{\Phi}(x_i)\\
&\leq \left(\frac{-\beta}{2} - \frac{1}{\Delta t}\right)\max_{x_i\in\Omega^N} |\mathcal{L}^N\widetilde{\Phi}(x_i)| \pm \mathcal{L}^N\widetilde{\Phi}(x_i)\\
&\leq -|\mathcal{L}^N\widetilde{\Phi}(x_i)| \pm \mathcal{L}^N\widetilde{\Phi}(x_i)\\
&\leq 0.
\end{aligned}$$

The proof is completed by applying Lemma 4.1. □

Theorem 4.1. *Let* $\widetilde{\psi}_i$ *is the approximate solution of the fully discretized scheme (3.2). Then, at the* $(j+1)$*-th time level, the following error estimate holds*

$$|u(x_i, t_{j+1}) - \widetilde{\psi}_i| \leq CN^{-1}\ln N, \quad i = 0, 1, \ldots, N.$$

Proof. To prove this, we decompose the solution $\widetilde{\psi}_i$ as

$$\widetilde{\psi}_i = \widetilde{\psi}_i^r + \widetilde{\psi}_i^s,$$

where $\widetilde{\psi}_i^r$ and $\widetilde{\psi}_i^s$ satisfy the following inhomogeneous and homogeneous problems, respectively

$$\begin{aligned}
&\mathcal{L}^N \widetilde{\psi}_i^r = \widetilde{g}(x_{i-1/2}) \text{ in } \mathcal{D}^{N,M}, \quad \widetilde{\psi}_i^r = u_r(x_i, t_{j+1}) \text{ on } \Gamma^{N,M},\\
&\mathcal{L}^N \widetilde{\psi}_i^s = 0 \text{ in } \mathcal{D}^{N,M}, \quad \widetilde{\psi}_i^s = u_s(x_i, t_{j+1}) \text{ on } \Gamma^{N,M}.
\end{aligned}$$

The nodal error is given by

$$\nu_{i,j+1} = u(x_i, t_{j+1}) - \widetilde{\psi}_i \approx (u_r(x_i, t_{j+1}) - \widetilde{\psi}_i^r) + (u_s(x_i, t_{j+1}) - \widetilde{\psi}_i^s).$$

Now we will estimate the errors on each component separately. From the differential equation and the result given in [12], we obtain

$$|\mathcal{L}^N(u_r(x_i, t_{j+1}) - \widetilde{\psi}_i^r)| \le C\varepsilon(x_{i+1} - x_{i-1})|u_r'''(x_i, t_{j+1})|, \quad 0 \le i \le N.$$

The value of $|u_r'''(x_i, t_{j+1})|$ can be estimated by using Theorem 3.3 and the fact $x_{i+1} - x_{i-1} \le 4N^{-1}$, to obtain

$$|\mathcal{L}^N(u_r(x_i, t_{j+1}) - \widetilde{\psi}_i^r)| \le CN^{-1}, \quad 0 \le i \le N.$$

An application of Lemma 4.2 gives the following estimate

$$|u_r(x_i, t_{j+1}) - \widetilde{\psi}_i^r| \le CN^{-1}, \quad 0 \le i \le N. \tag{4.1}$$

The error in the singular component is obtained by considering $\tau = 1/2$ and $\tau = \tau^*\sqrt{\varepsilon}\,\ln N$ separately. In the former case the mesh is uniform and $\tau^*\sqrt{\varepsilon}\,\ln N \ge \frac{1}{2}$. Then, using the classical argument, we obtain

$$|\mathcal{L}^N(u_s(x_i, t_{j+1}) - \widetilde{\psi}_i^s)| \le C\varepsilon(x_{i+1} - x_{i-1})|u_s'''(x_i, t_{j+1})|.$$

Again the application of Theorem 3.3 and the fact that $x_{i+1} - x_{i-1} = 2N^{-1}$, gives

$$|\mathcal{L}^N(u_s(x_i, t_{j+1}) - \widetilde{\psi}_i^s)| \le CN^{-1}\varepsilon^{-1/2},$$

which gives

$$|\mathcal{L}^N(u_s(x_i, t_{j+1}) - \widetilde{\psi}_i^s)| \le CN^{-1}\ln N.$$

Using Lemma 4.2, we obtain

$$|u_s(x_i, t_{j+1}) - \widetilde{\psi}_i^s| \le CN^{-1}\ln N. \tag{4.2}$$

In the latter case, depending on the mesh spacing, different arguments are used to obtain an estimate on $|u_s(x_i, t_{j+1}) - \widetilde{\psi}_i^s|$. For x_i in the subinterval $[0, \tau)$ the classical argument as used above gives

$$|\mathcal{L}^N(u_s(x_i, t_{j+1}) - \widetilde{\psi}_i^s)| \le C\varepsilon(x_{i+1} - x_{i-1})|u_s'''(x_i, t_{j+1})|, \quad 0 \le i \le \frac{N}{2}.$$

Since the mesh width is $\frac{2\tau}{N}$ and $|u_s'''(x_i, t_{j+1})| \le C\varepsilon^{-3/2}$, therefore

$$|\mathcal{L}^N(u_s(x_i, t_{j+1}) - \widetilde{\psi}_i^s)| \le CN^{-1}\frac{\tau}{\sqrt{\varepsilon}} \le CN^{-1}\ln N, \quad 0 \le i \le \frac{N}{2}. \tag{4.3}$$

On the other hand, as $|\delta^2 u_s(x_i,t_{j+1})| \leq \max_{x\in[x_{i-1},x_{i+1}]} |(u_s)''(x_i,t_{j+1})|$, for $x_i \in [\tau,1]$, we have

$$|\mathcal{L}^N(u_s(x_i,t_{j+1}) - \widetilde{\psi}_i^s)| \leq C\varepsilon \max_{x\in[x_{i-1},x_{i+1}]} |(u_s)''(x_i,t_{j+1})|, \quad \frac{N}{2}+1 \leq i \leq N.$$

Using the estimates

$$|\mathcal{L}^N(u_s(x_i,t_{j+1}) - \widetilde{\psi}_i^s)| \leq C \begin{cases} e^{-\sqrt{\beta}(x_{i-1})/\sqrt{\varepsilon}}, & \text{if} \quad x_i \leq \frac{1}{2}, \\ e^{-\sqrt{\beta}(1-x_i)/\sqrt{\varepsilon}}, & \text{if} \quad x_i > \frac{1}{2}. \end{cases}$$

Now for $x_i \leq 1/2$, $x_i = \tau$ or $x_i > \tau$. If $x_i > \tau$ then $x_{i-1} \geq \tau$ and so

$$e^{-\sqrt{\beta}(x_{i-1})/\sqrt{\varepsilon}} \leq e^{-\sqrt{\beta}\tau/\sqrt{\varepsilon}} \leq N^{-1}.$$

Since $x_{i-1} = \tau - \frac{2\tau}{N}$ for $x_i = \tau$, so

$$\begin{aligned} e^{-\sqrt{\beta}(x_{i-1})/\sqrt{\varepsilon}} &= e^{-\sqrt{\beta}\left(\tau-\frac{2\tau}{N}\right)/\sqrt{\varepsilon}} \\ &\leq e^{-\ln N} . \quad e^{2N^{-1}\ln N} \\ &= N^{-1}\left(N^{1/N}\right)^2 \leq CN^{-1}. \end{aligned}$$

It follows that

$$|\mathcal{L}^N(u_s(x_i,t_{j+1}) - \widetilde{\psi}_i^s)| \leq CN^{-1}, \quad \frac{N}{2}+1 \leq i \leq N. \tag{4.4}$$

The same result is obtained for the case of $x_i > 1/2$. Combining (4.3) and (4.4) gives

$$|\mathcal{L}^N(u_s(x_i,t_{j+1}) - \widetilde{\psi}_i^s)| \leq CN^{-1}\ln N, \quad 0 \leq i \leq N.$$

Thus the discrete minimum principle gives

$$|u_s(x_i,t_{j+1}) - \widetilde{\psi}_i^s| \leq CN^{-1}\ln N, \quad 0 \leq i \leq N. \tag{4.5}$$

The inequalities (4.1), (4.5), and the triangle inequality, give the required result. □

Theorem 4.2 (Main Result)**.** *The solution $\widetilde{\psi}_i$ of the fully discretized scheme (3.2) converges uniformly to the solution $\psi(x,t)$ of (1.1) and the error estimate is given by*

$$|\psi(x_i,t_j) - \widetilde{\psi}_i| \leq C((\Delta t)^2 + N^{-1}\ln N), \quad i = 0,1,\ldots,N,\ j = 0,1,\ldots,M.$$

Proof. The proof immediately follows from Theorem 3.1 and Theorem 4.1. □

5. Numerical Illustrations

To verify the theoretical results, computational results for three test problems are presented in the form of tables and graphs. For each ε, to measure the accuracy of the method, the maximum absolute error is obtained as

$$e_\varepsilon^{N,M} = \max_j \left(\max_i |\widetilde{\psi}_{2i}^{2N,2M} - \widetilde{\psi}_i^{N,M}| \right),$$

Table 1. $e_\varepsilon^{N,M}$, $e^{N,M}$, $q_\varepsilon^{N,M}$ and $q^{N,M}$ for Example 5.1 for $p = 1$

	Number of grid points					
ε	32	64	128	256	512	1024
2^0	$5.16(e-04)$	$2.69(e-04)$	$1.38(e-04)$	$6.95(e-05)$	$3.49(e-05)$	$1.75(e-05)$
	0.94	0.96	0.99	0.99	0.99	
2^{-4}	$6.42(e-03)$	$2.56(e-03)$	$9.98(e-04)$	$4.09(e-04)$	$1.79(e-04)$	$6.20(e-05)$
	1.33	1.36	1.29	1.19	1.53	
2^{-8}	$1.22(e-02)$	$5.68(e-03)$	$2.70(e-03)$	$1.31(e-03)$	$6.73(e-04)$	$3.41(e-04)$
	1.10	1.07	1.04	0.96	0.98	
2^{-12}	$1.24(e-02)$	$5.98(e-03)$	$2.92(e-03)$	$1.58(e-03)$	$8.37(e-04)$	$4.36(e-04)$
	1.05	1.03	0.89	0.92	0.94	
2^{-16}	$1.24(e-02)$	$5.99(e-03)$	$2.94(e-03)$	$1.60(e-03)$	$8.56(e-04)$	$4.49(e-04)$
	1.05	1.03	0.88	0.90	0.93	
2^{-20}	$1.24(e-02)$	$5.99(e-03)$	$2.94(e-03)$	$1.60(e-03)$	$8.57(e-04)$	$4.50(e-04)$
	1.05	1.03	0.88	0.90	0.93	
$\vdots$	$\vdots$	$\vdots$	$\vdots$	$\vdots$	$\vdots$	
2^{-32}	$1.24(e-02)$	$5.99(e-03)$	$2.94(e-03)$	$1.60(e-03)$	$8.57(e-04)$	$4.50(e-04)$
	1.05	1.03	0.88	0.90	0.93	
$e^{N,M}$	$1.24(e-02)$	$5.99(e-03)$	$2.94(e-03)$	$1.60(e-03)$	$8.57(e-04)$	$4.50(e-04)$
$q^{N,M}$	1.05	1.03	0.88	0.90	0.93	

Table 2. $e_\varepsilon^{N,M}$ and $q_\varepsilon^{N,M}$ for Example 5.1 for $\varepsilon = 2^{-10}$ and different values of p

	Number of grid points					
p	32	64	128	256	512	1024
2	$1.11(e-02)$	$5.56(e-03)$	$3.07(e-03)$	$1.69(e-03)$	$8.96(e-04)$	$4.64(e-04)$
	1.00	0.86	0.86	0.92	0.95	
4	$1.11(e-02)$	$5.59(e-03)$	$3.26(e-03)$	$1.81(e-03)$	$9.60(e-04)$	$4.97(e-04)$
	0.99	0.78	0.85	0.91	0.95	
6	$1.11(e-02)$	$5.86(e-03)$	$3.30(e-03)$	$1.81(e-03)$	$9.53(e-04)$	$4.92(e-04)$
	0.92	0.83	0.87	0.93	0.95	
8	$1.11(e-02)$	$5.91(e-03)$	$3.29(e-03)$	$1.77(e-03)$	$9.29(e-04)$	$4.77(e-04)$
	0.91	0.85	0.89	0.93	0.96	
10	$1.13(e-02)$	$6.01(e-03)$	$3.23(e-03)$	$1.73(e-03)$	$9.00(e-04)$	$4.60(e-04)$
	0.91	0.89	0.90	0.94	0.97	

where $\widetilde{\psi}_i^{N,M}$ and $\widetilde{\psi}_{2i}^{2N,2M}$ are the numerical solutions obtained at j-th level on $\mathcal{D}^{N,M}$, and $\mathcal{D}^{2N,2M}$ respectively. Note that the values of τ defined in Section 3 are different when we take N and $2N$ partitions in the spatial direction, which results in the mismatching in the nodal points. Thus, comparing the solutions using the double mesh principle will not work. To fix this issue, the mesh $\mathcal{D}^{2N,2M}$ is obtained by the mesh $\mathcal{D}^{N,M}$ by inserting a new nodal point between two consecutive points (using the collocation method). The ε-uniform point-wise error is calculated using

$$e^{N,M} = \max_{\varepsilon} e_\varepsilon^{N,M}.$$

Furthermore, the order of convergence $q_\varepsilon^{N,M}$ and the ε-uniform order of convergence $q^{N,M}$ are computed as

$$q_\varepsilon^{N,M} = \log_2\left(\frac{e_\varepsilon^{N,M}}{e_\varepsilon^{2N,2M}}\right), \text{ and } q^{N,M} = \log_2\left(\frac{e^{N,M}}{e^{2N,2M}}\right).$$

The following three test problems are encountered.

Example 5.1. First, we consider

$$-\frac{\partial\psi(x,t)}{\partial t}+\varepsilon\frac{\partial^2\psi(x,t)}{\partial x^2}+x^p\frac{\partial\psi(x,t)}{\partial x}-\psi(x,t)=x^2-1,\ (x,t)\in\mathcal{D},$$
$$\psi(x,0)=0,\ 0\le x\le 1,\quad \psi(0,t)=t,\ \psi(1,t)=0,\ 0\le t\le 1.$$

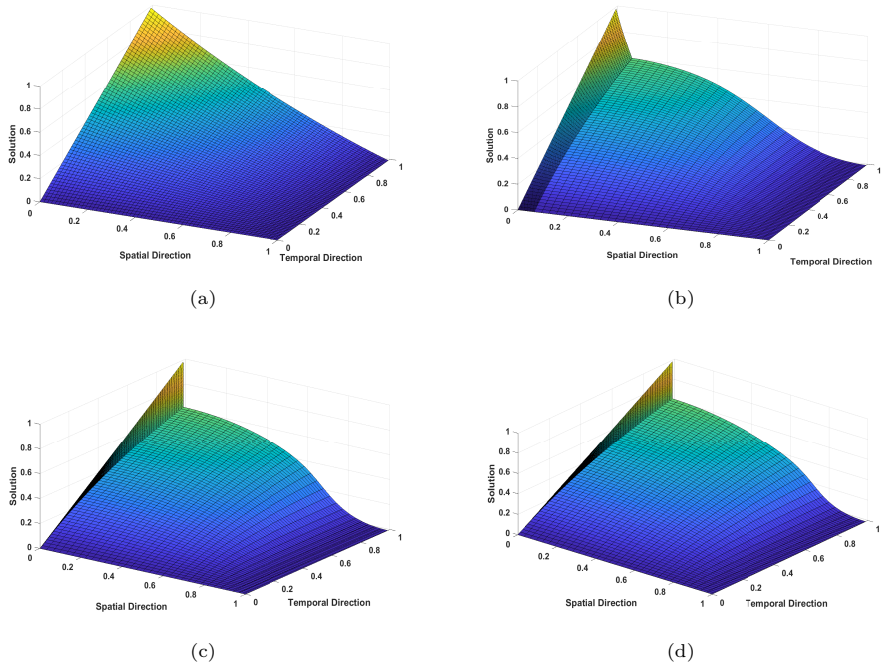

Figure 1. Numerical solution profiles for Example 5.1 for (a) $\varepsilon=1, p=1$ (b) $\varepsilon=2^{-6}, p=3$ (c) $\varepsilon=2^{-12}, p=5$ and (d) $\varepsilon=2^{-18}, p=7$.

Example 5.2. Next, we consider

$$-\frac{\partial\psi(x,t)}{\partial t}+\varepsilon\frac{\partial^2\psi(x,t)}{\partial x^2}+(2-x^2)x^p\frac{\partial\psi(x,t)}{\partial x}-(1+x)\psi(x,t)=10t^2e^{-t}x(x-1),$$
$$(x,t)\in\mathcal{D},$$
$$\psi(x,0)=1-x,\ 0\le x\le 1,\quad \psi(0,t)=1+t^2,\ \psi(1,t)=0,\ 0\le t\le 1.$$

Example 5.3. Finally, we consider

$$-\frac{\partial\psi(x,t)}{\partial t}+\varepsilon\frac{\partial^2\psi(x,t)}{\partial x^2}+x^p\frac{\partial\psi(x,t)}{\partial x}-\psi(x,t)=x^2-1,\ (x,t)\in\mathcal{D},$$
$$\psi(x,0)=(1-x)^2,\ 0\le x\le 1,\quad \psi(0,t)=1+t^2,\ \psi(1,t)=0,\ 0\le t\le 1.$$

The numerical results presented in the tables confirm the theoretical results proved in Theorem 4.2, which clearly show the ε-uniform convergence of the method. All the results presented in Tables 1-4 and in Table 7 are obtained by taking $M=N$. Also, We have used 64 points in both directions to plot all the graphs. Tables 5 and

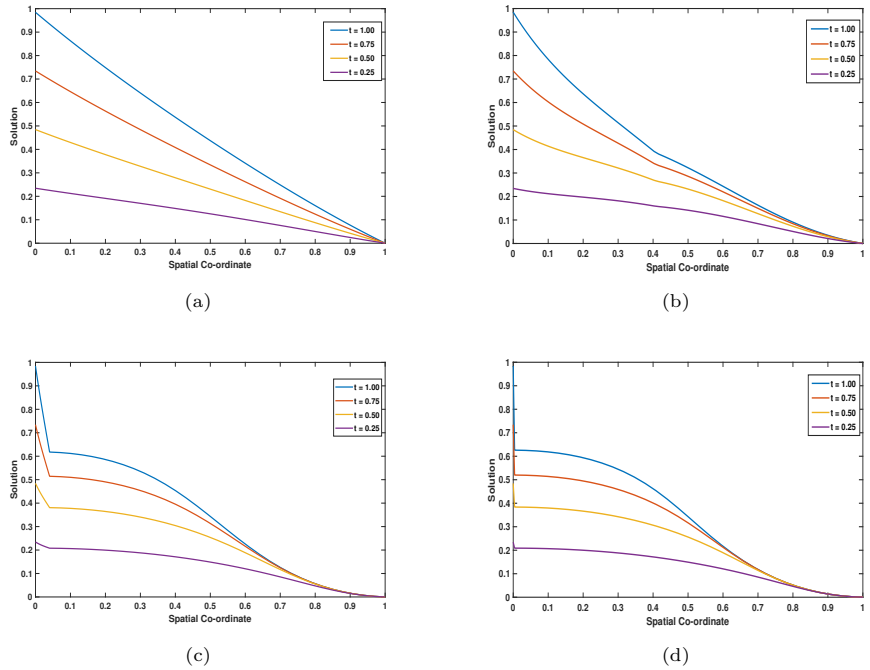

Figure 2. Numerical solution profiles for $p = 2$ at different time levels for Example 5.1 for (a) $\varepsilon = 1$ (b) $\varepsilon = 0.1$ (c) $\varepsilon = 0.01$ and (d) $\varepsilon = 0.001$.

Table 3. $e_\varepsilon^{N,M}$, $e^{N,M}$, $q_\varepsilon^{N,M}$ and $q^{N,M}$ for Example 5.2 for $p = 1$

	Number of grid points					
ε	32	64	128	256	512	1024
2^0	$2.16(e-03)$	$1.03(e-03)$	$4.94(e-04)$	$2.44(e-04)$	$1.21(e-04)$	$6.00(e-05)$
	1.07	1.06	1.02	1.01	1.01	
2^{-4}	$5.48(e-03)$	$3.54(e-03)$	$1.80(e-03)$	$9.06(e-04)$	$4.55(e-04)$	$2.28(e-04)$
	0.63	0.97	0.99	0.99	1.00	
2^{-8}	$5.13(e-02)$	$2.43(e-02)$	$1.14(e-02)$	$5.19(e-03)$	$2.33(e-03)$	$1.02(e-03)$
	1.08	1.09	1.13	1.15	1.19	
2^{-12}	$7.45(e-02)$	$3.76(e-02)$	$1.80(e-02)$	$8.82(e-03)$	$4.41(e-03)$	$2.21(e-03)$
	0.99	1.06	1.03	1.00	1.00	
2^{-16}	$7.78(e-02)$	$4.16(e-02)$	$2.12(e-02)$	$1.02(e-02)$	$4.69(e-03)$	$2.26(e-03)$
	0.90	0.97	1.05	1.12	1.05	
2^{-20}	$7.81(e-02)$	$4.20(e-02)$	$2.18(e-02)$	$1.11(e-02)$	$5.47(e-03)$	$2.58(e-03)$
	0.89	0.95	0.97	1.02	1.08	
$\vdots$	$\vdots$	$\vdots$	$\vdots$	$\vdots$	$\vdots$	
2^{-32}	$7.81(e-02)$	$4.21(e-02)$	$2.19(e-02)$	$1.12(e-02)$	$5.63(e-03)$	$2.83(e-03)$
	0.89	0.94	0.97	0.99	0.99	
$e^{N,M}$	$7.81(e-02)$	$4.21(e-02)$	$2.19(e-02)$	$1.12(e-02)$	$5.63(e-03)$	$2.83(e-03)$
$q^{N,M}$	0.89	0.94	0.97	0.99	0.99	

6 show the accuracy in space and time separately for all Examples. To observe the change in the boundary layer width with respect to the parameter and to show the physical phenomenon of the solution, the surface plots (refer to Figs. 1, 3, and 5) have been presented. From these figures, one can observe that the solution exhibits

Table 4. $e_\varepsilon^{N,M}$ and $q_\varepsilon^{N,M}$ for Example 5.2 for $\varepsilon = 2^{-10}$ and different values of p

	Number of grid points					
p	32	64	128	256	512	1024
2	$5.44(e-02)$	$2.75(e-02)$	$1.42(e-02)$	$7.26(e-03)$	$3.64(e-03)$	$1.81(e-03)$
	0.98	0.95	0.97	1.00	1.00	
4	$5.34(e-02)$	$2.72(e-02)$	$1.42(e-02)$	$7.23(e-03)$	$3.63(e-03)$	$1.81(e-03)$
	0.97	0.94	0.97	0.99	1.00	
6	$5.34(e-02)$	$2.72(e-02)$	$1.42(e-02)$	$7.23(e-03)$	$3.63(e-03)$	$1.81(e-03)$
	0.97	0.94	0.97	0.99	1.00	
8	$5.34(e-02)$	$2.72(e-02)$	$1.42(e-02)$	$7.23(e-03)$	$3.63(e-03)$	$1.81(e-03)$
	0.97	0.94	0.97	0.99	1.00	
10	$5.34(e-02)$	$2.72(e-02)$	$1.42(e-02)$	$7.23(e-03)$	$3.63(e-03)$	$1.81(e-03)$
	0.97	0.94	0.97	0.99	1.00	

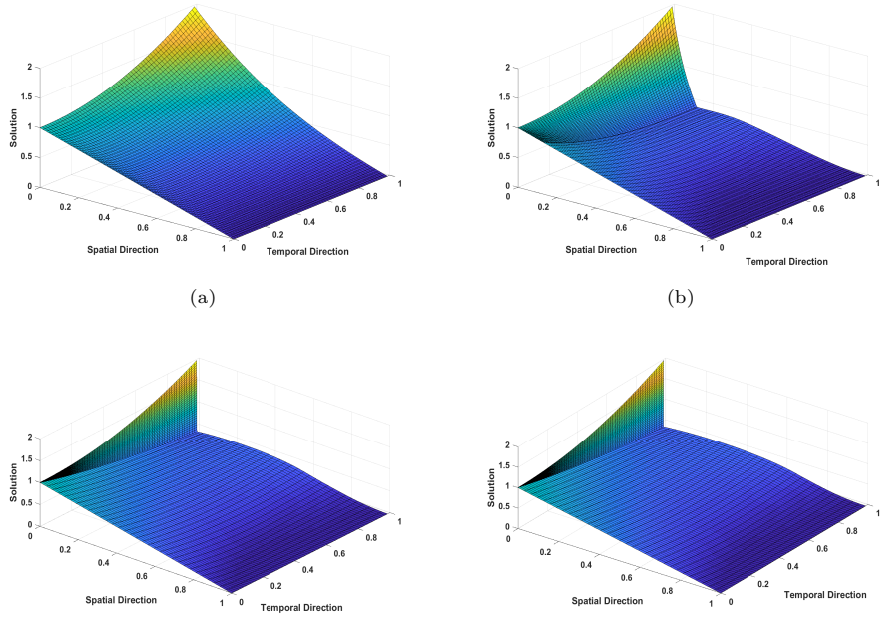

(a) (b)

(c) (d)

Figure 3. Numerical solution profiles for Example 5.2 for (a) $\varepsilon = 1, p = 1$ (b) $\varepsilon = 2^{-6}, p = 3$ (c) $\varepsilon = 2^{-12}, p = 5$ and (d) $\varepsilon = 2^{-18}, p = 7$.

a boundary layer at $x = 0$ for small ε, and the boundary layer width decreases as the parameter decreases. The solution behavior for different time levels is also drawn (refer to Figs. 2 and 4). A comparison of the results for Example 5.3 with those of [2] is presented in Table 7.

6. Conclusion

We have proposed an implicit parameter-uniform numerical scheme of $\mathcal{O}((\Delta t)^2 + N^{-1} \ln N)$ for SPBVPs exhibiting a boundary turning point. The presence of ε and the boundary turning point make these problems more difficult to solve numerically.

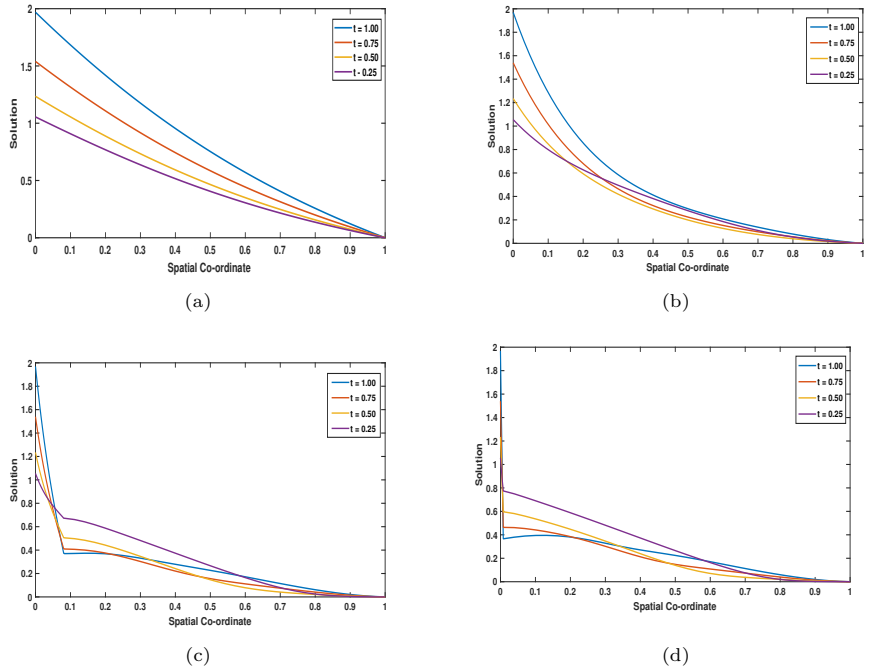

Figure 4. Numerical solution profiles for $p = 2$ at different time levels for Example 5.2 for (a) $\varepsilon = 1$ (b) $\varepsilon = 0.1$ (c) $\varepsilon = 0.01$ and (d) $\varepsilon = 0.001$.

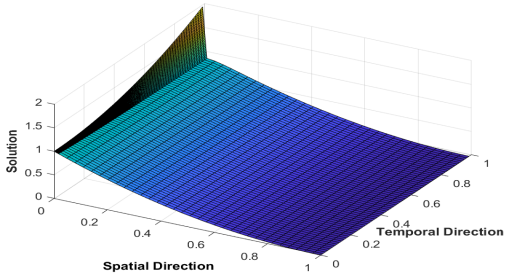

Figure 5. Surface plots of the numerical solution for Example 5.3 for $\varepsilon = 2^{-8}, p = 1$.

The uniform convergence is proved through a rigorous analysis. The method can also be extended to the reaction-diffusion SPBVPs whose solution exhibits parabolic boundary layers on both sides of the domain as ε approaches zero. The analysis is also valid for $p = 0$ when the solution generally has a different kind of layer than the layer that appears in our problem. Three test examples are encountered to check the accuracy and efficiency of the method.

Acknowledgments.

The authors are grateful to the unknown reviewers for their insightful observations leading to the improvement of the manuscript.

Table 5. The maximum absolute errors and the orders of convergence in the spatial direction for all examples for $p = 3$ and $M = 64$

	N					
ε	32	64	128	256	512	1024
Example 5.1						
2^0	$1.22(e-3)$	$6.36(e-4)$	$3.25(e-4)$	$1.64(e-4)$	$8.24(e-5)$	$4.13(e-5)$
	0.94	0.97	0.99	0.99	0.99	
2^{-4}	$1.41(e-2)$	$5.70(e-3)$	$2.36(e-3)$	$1.00(e-4)$	$4.33(e-5)$	$1.89(e-5)$
	1.30	1.27	1.24	1.21	1.20	
2^{-8}	$2.17(e-2)$	$1.07(e-2)$	$5.18(e-3)$	$2.54(e-3)$	$1.14(e-3)$	$5.08(e-4)$
	1.02	1.05	1.03	1.15	1.17	
2^{-12}	$2.21(e-2)$	$1.12(e-2)$	$5.66(e-3)$	$2.87(e-3)$	$1.39(e-3)$	$6.91(e-4)$
	0.98	0.98	0.98	1.05	1.01	
2^{-16}	$2.21(e-2)$	$1.12(e-2)$	$5.66(e-3)$	$2.87(e-3)$	$1.39(e-3)$	$6.91(e-4)$
	0.98	0.98	0.98	1.05	1.01	
Example 5.2						
2^0	$2.12(e-3)$	$1.02(e-3)$	$4.94(e-4)$	$2.44(e-4)$	$1.21(e-4)$	$6.01(e-5)$
	1.05	1.05	1.02	1.01	1.01	
2^{-4}	$2.78(e-3)$	$1.25(e-3)$	$6.40(e-4)$	$3.25(e-4)$	$1.64(e-4)$	$8.22(e-5)$
	1.15	0.96	0.98	0.99	1.00	
2^{-8}	$5.11(e-2)$	$2.55(e-2)$	$1.26(e-2)$	$6.06(e-3)$	$2.88(e-3)$	$1.36(e-3)$
	1.00	1.00	1.06	1.07	1.08	
2^{-12}	$5.60(e-2)$	$2.76(e-2)$	$1.41(e-2)$	$7.38(e-3)$	$3.80(e-3)$	$1.93(e-3)$
	1.02	0.97	0.93	0.96	0.98	
2^{-16}	$5.69(e-2)$	$2.83(e-2)$	$1.40(e-2)$	$6.94(e-3)$	$3.56(e-3)$	$1.80(e-3)$
	1.01	1.01	1.01	0.96	0.98	
Example 5.3						
2^0	$4.13(e-3)$	$2.02(e-3)$	$9.85(e-4)$	$4.88(e-4)$	$2.42(e-4)$	$1.20(e-4)$
	1.03	1.04	1.01	1.01	1.01	
2^{-4}	$1.93(e-2)$	$7.97(e-3)$	$3.51(e-3)$	$1.64(e-3)$	$9.28(e-4)$	$4.98(e-4)$
	1.27	1.18	1.10	0.82	0.90	
2^{-8}	$3.30(e-2)$	$1.75(e-2)$	$8.92(e-3)$	$4.47(e-3)$	$2.22(e-3)$	$1.12(e-3)$
	0.91	0.97	1.00	1.01	0.99	
2^{-12}	$3.10(e-2)$	$1.77(e-2)$	$9.84(e-3)$	$5.42(e-3)$	$2.91(e-3)$	$1.54(e-3)$
	0.81	0.85	0.86	0.90	0.92	
2^{-16}	$3.11(e-2)$	$1.78(e-2)$	$9.84(e-3)$	$5.43(e-3)$	$2.80(e-3)$	$1.43(e-3)$
	0.80	0.85	0.86	0.95	0.97	

References

[1] L. Bobisud, *Second-order linear parabolic equations with a small parameter*, Arch. Rational Mech. Anal., 1968, 27, 385–397.

[2] R. K. Dunne, E. O'Riordan and G. I. Shishkin, *A fitted mesh method for a class of singularly perturbed parabolic problems with a boundary turning point*, Comput. Methods Appl. Math., 2003, 3, 361–372.

[3] P. A. Farrell, A. F. Hegarty, J. J. H. Miller, E. O'Riordan and G. I. Shishkin, *Robust Computational Techniques for Boundary Layers,* Chapman & Hall, London, 2000.

Table 6. The maximum absolute errors and the orders of convergence in the temporal direction for all examples for $p = 3$ and $N = 64$

	M					
ε	32	64	128	256	512	1024
Example 5.1						
2^{0}	$8.48(e-3)$	$2.02(e-3)$	$4.88(e-4)$	$1.20(e-4)$	$3.24(e-5)$	$8.15(e-6)$
	2.07	2.05	2.02	1.89	1.99	
2^{-4}	$4.49(e-2)$	$7.97(e-3)$	$1.64(e-3)$	$5.20(e-4)$	$1.15(e-4)$	$2.84(e-5)$
	2.49	2.28	1.66	2.17	2.02	
2^{-8}	$6.02(e-2)$	$1.75(e-2)$	$4.47(e-3)$	$1.12(e-3)$	$2.79(e-4)$	$7.08(e-5)$
	1.78	1.97	2.00	2.01	1.98	
2^{-12}	$5.78(e-2)$	$1.77(e-2)$	$5.26(e-3)$	$1.54(e-3)$	$4.33(e-4)$	$1.15(e-4)$
	1.71	1.75	1.77	1.83	1.91	
2^{-16}	$5.76(e-2)$	$1.78(e-2)$	$5.23(e-3)$	$1.37(e-3)$	$3.59(e-4)$	$9.21(e-5)$
	1.69	1.77	1.93	1.93	1.96	
Example 5.2						
2^{0}	$4.69(e-3)$	$1.04(e-3)$	$2.44(e-4)$	$6.14(e-5)$	$1.62(e-5)$	$4.23(e-6)$
	2.17	2.09	1.99	1.92	1.94	
2^{-4}	$1.61(e-2)$	$4.27(e-3)$	$1.12(e-3)$	$2.95(e-4)$	$7.64(e-5)$	$1.88(e-5)$
	1.91	1.93	1.92	1.95	2.02	
2^{-8}	$1.05(e-1)$	$2.35(e-2)$	$6.13(e-3)$	$1.56(e-3)$	$4.08(e-4)$	$1.01(e-4)$
	2.16	1.94	1.97	1.93	2.01	
2^{-12}	$1.15(e-1)$	$2.66(e-2)$	$5.91(e-3)$	$1.48(e-3)$	$3.80(e-4)$	$9.28(e-5)$
	2.11	2.17	2.00	1.96	2.03	
2^{-16}	$1.15(e-1)$	$2.66(e-2)$	$5.91(e-3)$	$1.48(e-3)$	$3.80(e-4)$	$9.28(e-5)$
	2.11	2.17	2.00	1.96	2.03	
Example 5.3						
2^{0}	$8.48(e-3)$	$2.02(e-3)$	$4.88(e-4)$	$1.20(e-4)$	$3.22(e-5)$	$8.20(e-6)$
	2.07	2.05	2.02	1.90	1.97	
2^{-4}	$4.49(e-2)$	$7.97(e-3)$	$1.64(e-3)$	$3.69(e-4)$	$9.24(e-5)$	$2.15(e-5)$
	2.49	2.28	2.15	2.00	2.10	
2^{-8}	$6.02(e-2)$	$1.75(e-2)$	$4.27(e-3)$	$1.12(e-3)$	$2.88(e-4)$	$7.28(e-5)$
	1.78	2.03	1.93	1.96	1.98	
2^{-12}	$5.78(e-2)$	$1.77(e-2)$	$5.42(e-3)$	$1.54(e-3)$	$4.26(e-4)$	$1.14(e-4)$
	1.71	1.71	1.81	1.85	1.90	
2^{-16}	$5.76(e-2)$	$1.78(e-2)$	$5.44(e-3)$	$1.58(e-3)$	$4.31(e-4)$	$1.12(e-4)$
	1.69	1.71	1.78	1.87	1.94	

Table 7. $e_{\varepsilon}^{N,M}$ for Example 5.3 for $p = 1$

		Number of grid points					
ε		8	16	32	64	128	256
2^{0}	[2]	$3.44(e-2)$	$2.01(e-2)$	$1.15(e-2)$	$5.95(e-3)$	$2.88(e-3)$	$1.26(e-3)$
	PM	$1.62(e-2)$	$7.82(e-3)$	$3.95(e-3)$	$1.97(e-3)$	$9.70(e-4)$	$4.84(e-4)$
2^{-2}	[2]	$2.89(e-2)$	$1.46(e-2)$	$7.23(e-3)$	$3.52(e-3)$	$1.64(e-3)$	$7.06(e-4)$
	PM	$5.31(e-3)$	$2.41(e-3)$	$1.15(e-3)$	$6.33(e-4)$	$3.31(e-4)$	$1.69(e-4)$
2^{-6}	[2]	$4.93(e-2)$	$2.93(e-2)$	$1.68(e-2)$	$9.18(e-3)$	$4.29(e-3)$	$1.84(e-3)$
	PM	$6.17(e-2)$	$2.82(e-2)$	$1.32(e-2)$	$6.17(e-3)$	$2.88(e-3)$	$1.36(e-3)$
2^{-12}	[2]	$6.11(e-2)$	$3.45(e-2)$	$1.85(e-2)$	$9.34(e-3)$	$4.45(e-3)$	$1.98(e-3)$
	PM	$4.52(e-2)$	$2.01(e-2)$	$8.29(e-3)$	$3.64(e-3)$	$1.72(e-3)$	$8.81(e-4)$

[4] V. Gupta and M. K. Kadalbajoo, *A layer adaptive B-spline collocation method for singularly perturbed one-dimensional parabolic problem with a boundary*

turning point, Numer. Methods Part. Diff. Eqn., 2011, 27, 1143–1164.

[5] T. C. Hanks, *Model relating heat-flow values near, and vertical velocities of mass transport beneath, oceanic rises*, J. Geophys Res., 1971, 76, 537–544.

[6] R. B. Kellogg and A. Tsan, *Analysis of some difference approximations for a singular perturbation problem without turning point*, Math. Comp., 1978, 32, 1025–1039.

[7] D. Kumar and P. Kumari, *A parameter-uniform numerical scheme for the parabolic singularly perturbed initial boundary value problems with large time delay*, J. Appl. Math. Comput., 2019, 159, 79–206.

[8] O. A. Ladyzhenskaya, V. A. Solonnikov and N. N. Ural'tseva, *Linear and Quasilinear Equations of Parabolic Type, Translations of Mathematical Monographs,* Vol. 23, American Mathematical Society, USA, 1968.

[9] T. Lin and R. Vulanović, *Uniform methods for semi linear problems with an attractive boundary turning point*, Novi Sad J. Math., 2001, 31, 99–114.

[10] V. D. Liseikin and V. E. Petrenko, *Adaptive-Invariant Method for Numerical Solution of Problems with Boundary and Internal Layers,* Novosibirsk, 1989.

[11] V. D. Liseikin, *The use of special transformations in the numerical solution of boundary layer problems*, USSR Comput. Math. Math. Phys., 1990, 30, 43–53.

[12] J. J. H. Miller, E. O'Riordan and G. I. Shishkin, *Fitted Numerical Methods for Singular Perturbation Problems,* World Scientific, Singapore, 1996.

[13] P. Rai and K. K. Sharma, *Singularly perturbed parabolic differential equations with turning point and retarded arguments*, J. Appl. Math., 2015, 45, 4.

[14] H. G. Roos, M. Stynes and L. Tobiska, *Numerical Methods for Singular Perturbed Differential Equations,* Springer-Verlag, New York, 1996.

[15] A. A. Samarskii, *Theory of Finite-Difference Approximations,* Moscow, 1989.

[16] H. Schlichting, *Boundary Layer Theory,* McGraw-Hill, New York, 1979.

[17] G. I. Shishkin, *Grid approximations to singularly perturbed parabolic equations with turning points*, Differ. Equn., 2001, 37, 1037–1050.

[18] R. Vulanović, *On numerical solution of a mildly nonlinear turning point problem*, Math. Model. Num. Anal., 1990, 24, 765–783.

[19] R. Vulanović and P. Lin, *Numerical solution of quasi linear attractive turning point problems*, Comput. Math. Appl., 1992, 23, 75–82.

[20] R. Vulanović and P. A. Farrell, *Continuous and numerical analysis of a multiple turning point problem*, SIAM J. Numer. Anal., 1993, 30, 1400–1418.